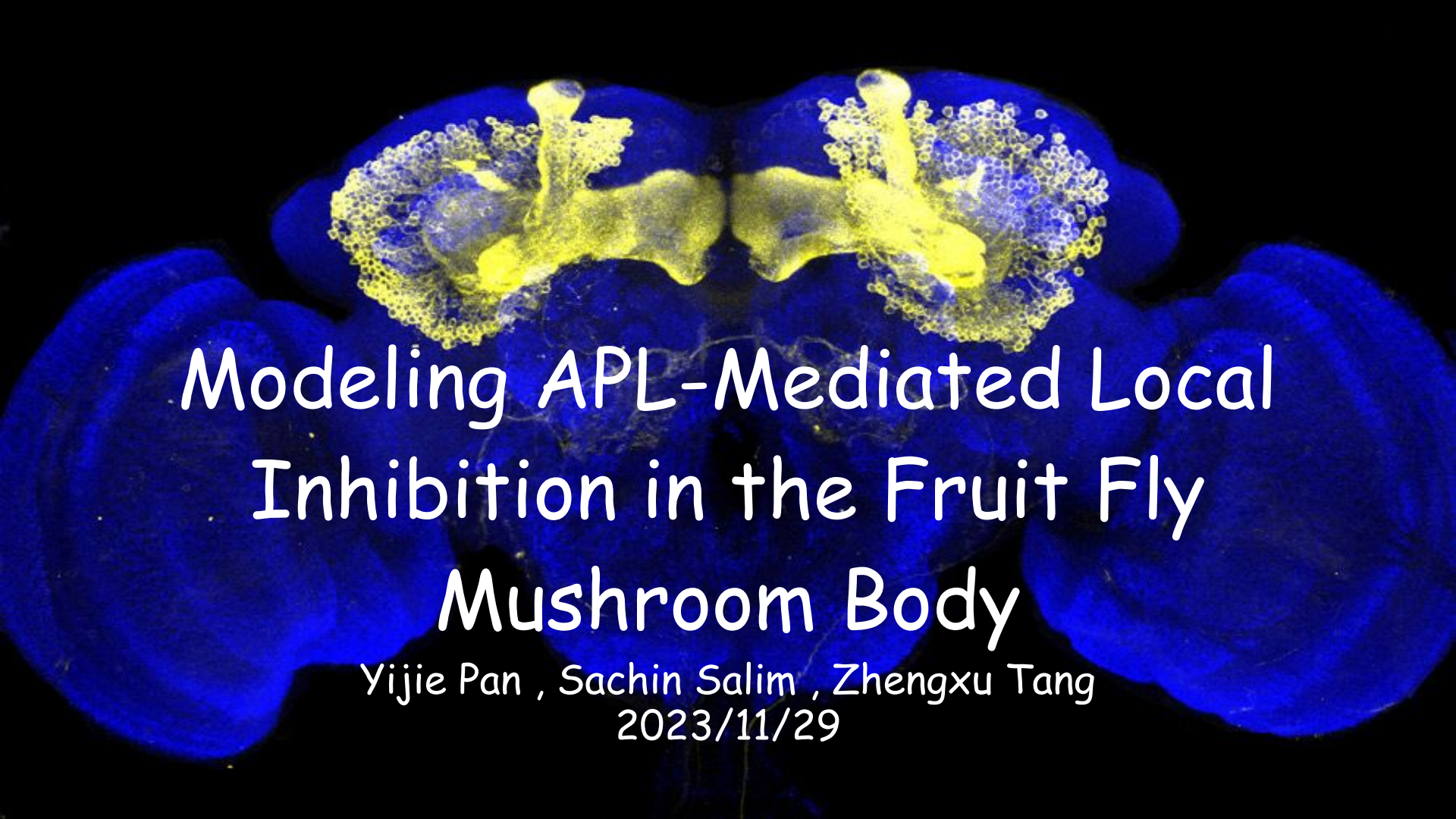

# Modeling APL-Mediated Local Inhibition in the Fruit Fly Mushroom Body

Yijie Pan , Sachin Salim , Zhengxu Tang

2023/11/29

# Introduction: Mushroom body

- Mushroom body is the learning hub of insects:
  - Mushroom body is the analog of hippocampus and cerebellum. The major type of neurons in mushroom body is Kenyon Cells (KC)
  - Kenyon Cells, receiving combinatory olfactory inputs, are the engrams of olfactory memory
  - Single odor activates an ensemble of Kenyon Cells. The sparsity of Kenyon Cells activity is critical for odor discrimination

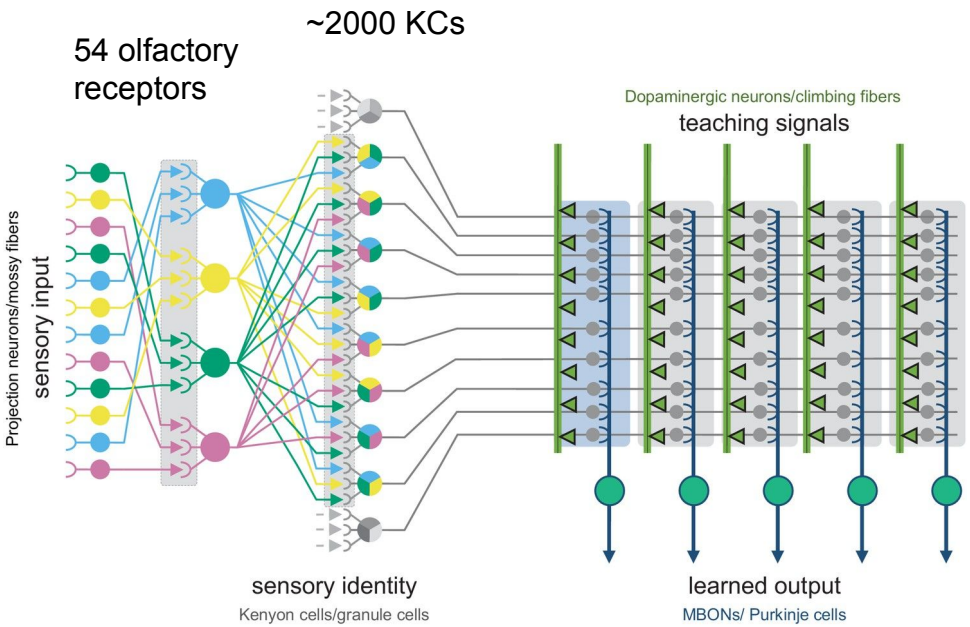


Li, Feng, et al. *Elife* (2020): e62576.

# Anterior Paired Lateral (APL) Neuron

- APL provides lateral inhibition in Mushroom body:
  - APL is a giant GABAergic interneuron (1 neuron per hemisphere)
  - APL neuron integrates inputs from all Kenyon Cells and delivers inhibitory feedback
  - APL is essential for olfactory discrimination
  - The inhibition from APL is not global

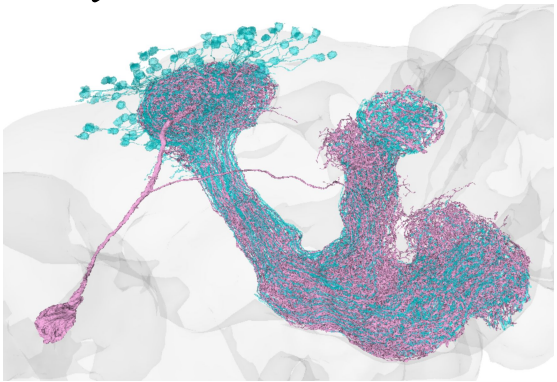


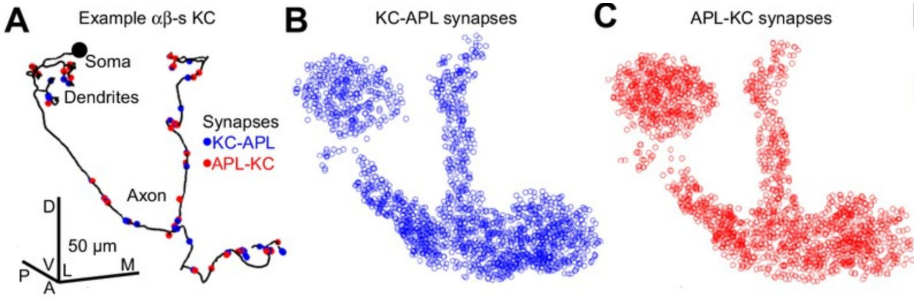


Amin, Hoger, et al. *Elife* (2020): e56954.

# Inhibition from APL is not Global

- APL provides local lateral inhibition
  - Not all KCs can inhibit each other by APL
  - APL don't have voltage gated ion channels for generating spikes

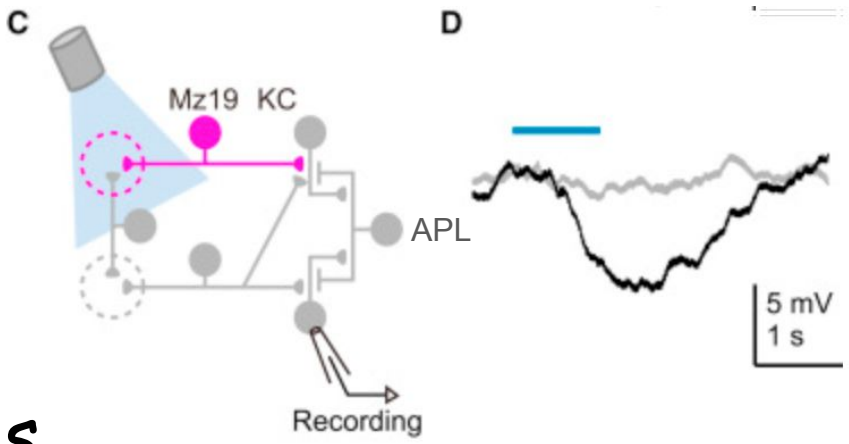


## What is the function of this local inhibition in the mushroom body?

Inada, Kengo, et al,*Neuron* 95.2 (2017): 357-367.

# Research Motivation and Objectives

- Our project aims to explore how APL imposes local inhibition on Kenyon Cells and how this inhibition affects olfactory perception and learning processes by building and analyzing computational models.

- We seek to understand the impact of APL's inhibitory mechanisms on the sparsity of sensory representations and the accuracy of learning by simulating these inhibitory processes.

# Previous Model

- Kennedy-MB model
  - Simplified LIF model for KCs
  - Input from experimental recording of 110 odors in ORNs
  - Uniform APL inhibition to all KCs
  - We aim to construct local inhibition model based on Kennedy-MB model

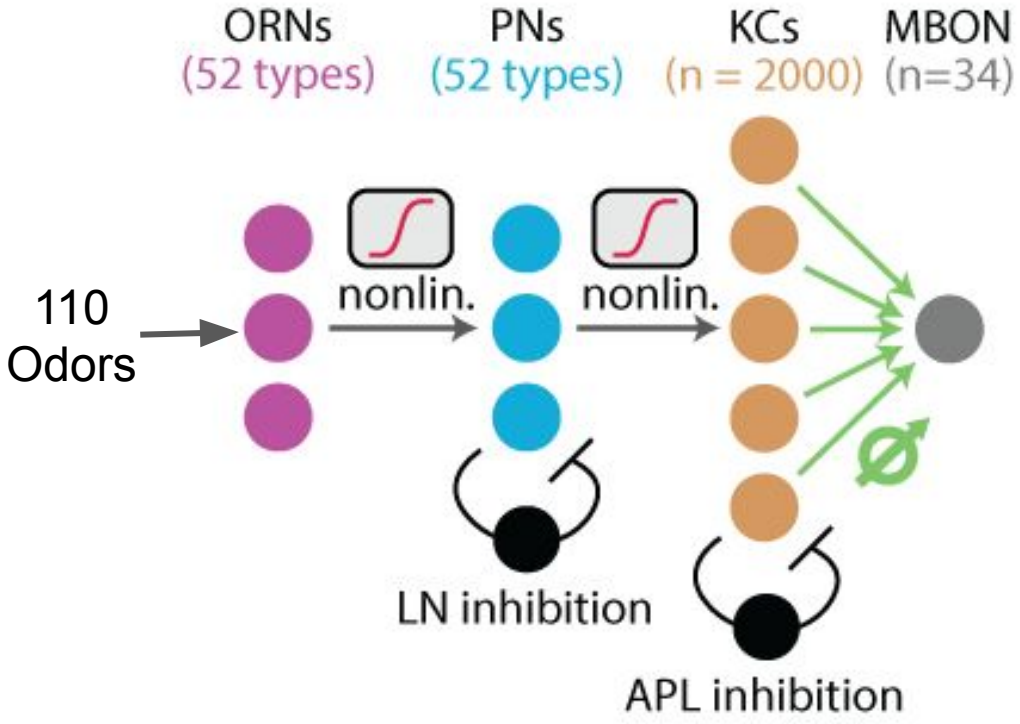


Kennedy, Ann. *bioRxiv* (2019): 783191.

# Modeling

# 2D KC grid

- KC receive excitatory input from Projection Neurons (PNs)
  - 2025 KCs arranged as 45*45 2-D KC matrix to simulate their spatial relationships
  - Each KC randomly receives 6 inputs from 23 PNs; PNs firing rate is from the Kennedy-MB model

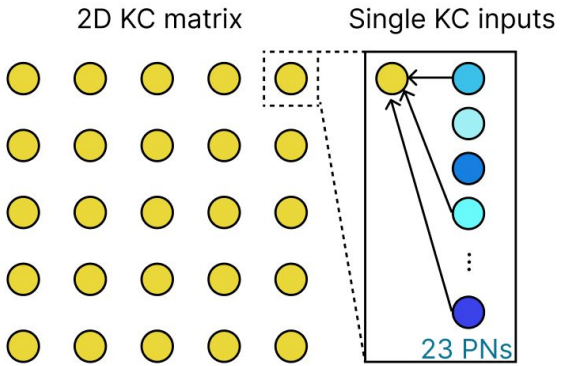


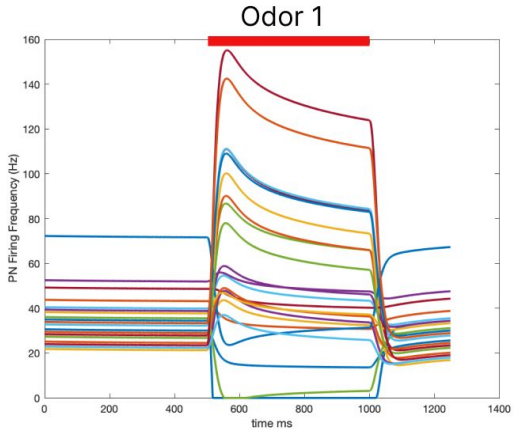

# PN-KC connectivity

- Each KC randomly sample 6 inputs from 23 PNs with replacement
  - Full(uniform)-random mode: All PN have the same weight to be sampled
  - Recent connectome analysis suggests closer KC share similar PN-KC connectivity
  - Local-random mode: The sampling weight of each PN is assigned by gaussian distributions in the 2-D KC space

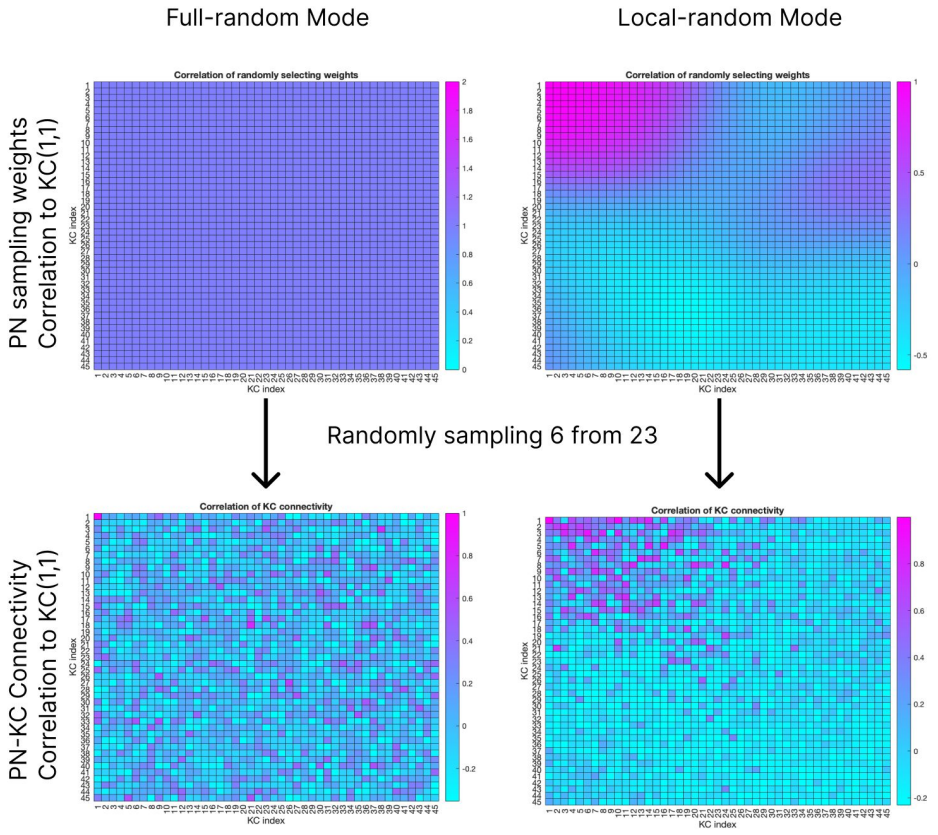

# Input current to KC

- At each time step, the input current to KC from PN is:

$$I_{i,j}(t) = A * w_{PN \rightarrow KC_{i,j}} * PN(t)$$

**w(PN->KC_i,j)**: Connectivity of KC i,j
**PN**: Firing rate of PN
***A***: Scaling factor

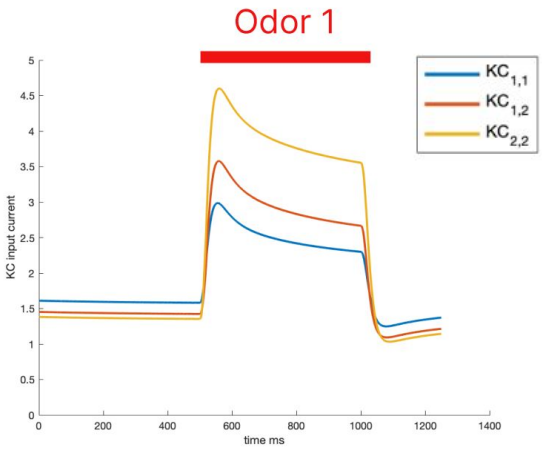


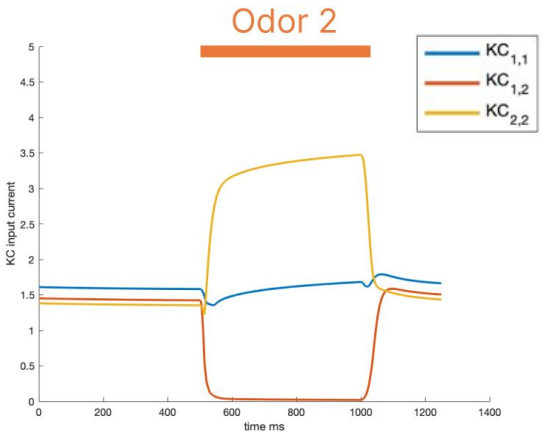

# Response of KC

- Each KC is implemented as Izhikevich 2D LIF model

$$\frac{dV}{dt} = 0.04\,V^2 + 5V + 140 - u + I$$

$$\frac{du}{dt} = a(bV - u)$$

Reset condition: If $V \geq 30$, then set $V = c$ and $u = u + d$

Parameter values: $a = 0.02$, $b = 0.2$, $c = -65$, $d = 8$

- For odor1, the input current to KC and the respective firing rates is visualized for a disconnected network
- It's compared between uniformly random and locally random connectivity between PN and KC

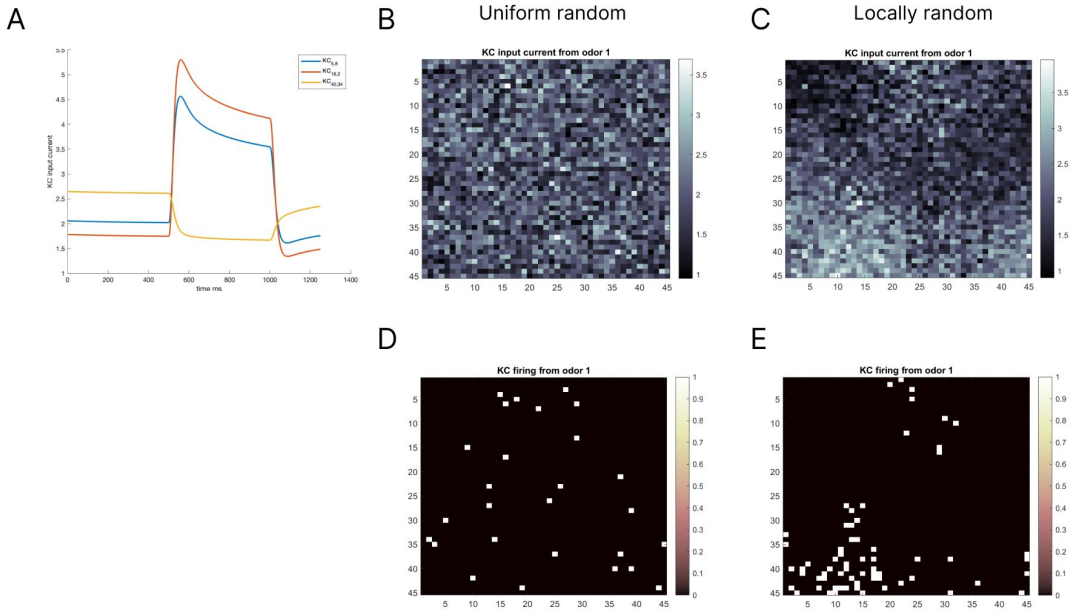


**Figure.** A) Input currents for odor 1 visualized for three sample KC
B, C) Input currents (max) visualized as a raster plot for all KC for uniform and local connectivity
D, E) The output firing rate of KC in a disconnected network

# KC Network - Connectivity

- The local forward/feedback inhibition of APL is modelled as a local lateral inhibition among Kenyon Cells
- The connection weight of a presynaptic-KC to a postsynaptic KC is modeled to decay with distance (as a gaussian function)

$$w_{syn}(r) = e^{-\frac{r^2}{2\sigma^2}}$$

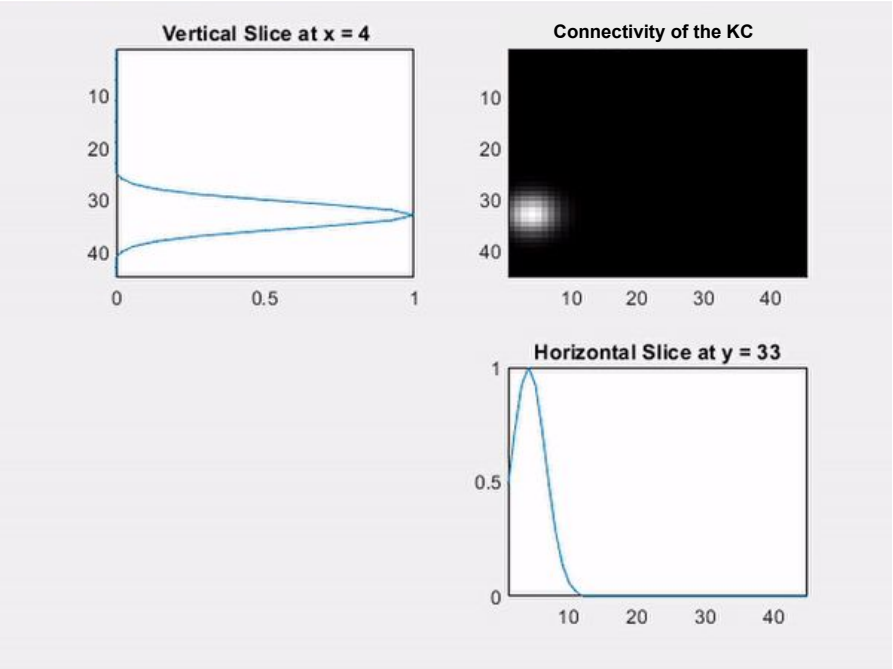


Each frame shows the connection weight of a given KC with other KCs

# KC Network - Connectivity

A) This figure illustrates how KC cells are connected in a 2D grid. The center cell (orange) is connected to all its neighboring cells but the strength decays with distance.

B) Adjacency matrix showing how the KC cells are connected (n=2025 [45x45], σ = 3)

C) Plot showing the connectivity strength decaying with spatial distance.

D) Adjacency matrix of a smaller network for visualization purpose (n=121 [11x11], σ = 1.5)

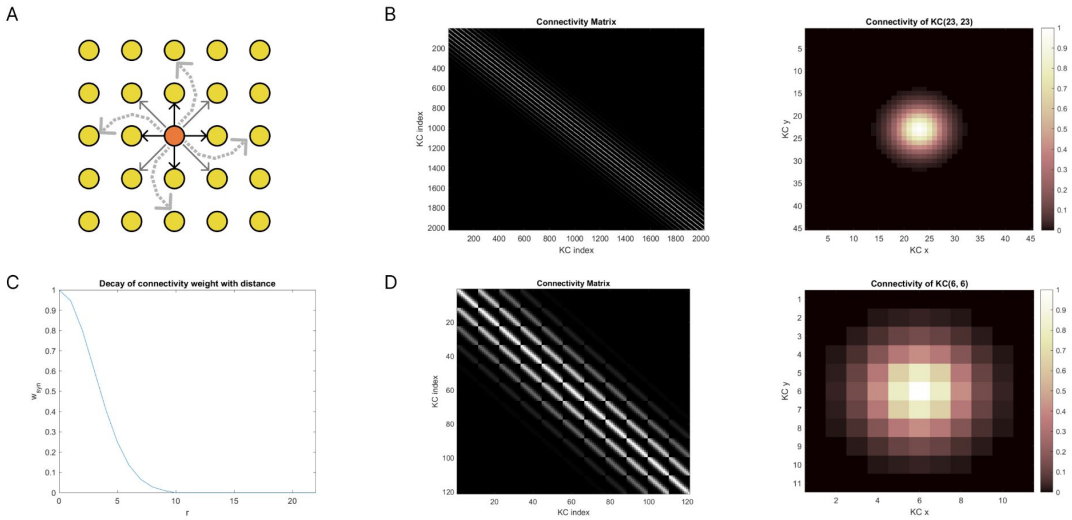

# KC Network - How connection params affect sparsity

These figures visualize how varying inhibition strength and range affects the sparsity of KC firing.
Analysed for odor 1, unif random,
A = 0.035, taus = 50.

A) visualizes the maximum input current across the time for each of the KC cells.

B) gsyn = 0 -> sparseness: 0.68

C) gsyn = -2, σ = 1 -> sparseness: 0.82

D) gsyn = -5, σ = 1 -> sparseness: 0.856

E) gsyn = -2, σ = 3 -> sparseness: 0.91

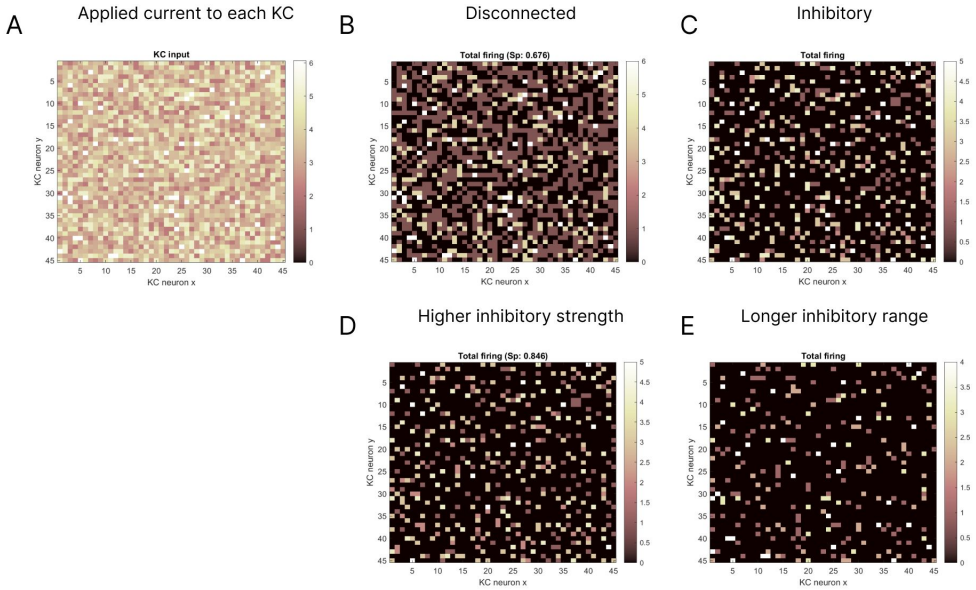


**Figure.** These figures visualize how varying inhibition strength and range affects the sparsity of KC firing. Analysed for odor 1, full random, A = 0.035, taus = 50. A) visualizes the maximum input current across the time for each of the KC cells. B) gsyn = 0, result: sparseness: 0.676 C) gsyn = -2, σ = 1, result: sparseness: 0.822 D) gsyn = -5, σ = 1, result: sparseness: 0.846 E) gsyn = -2, σ = 3, result: sparseness: 0.912

# Tuning parameter: Input strength

- In Kennedy-MB model, a model without APL have ~25% KC responding to a odor on average
- We randomly select 8 odors and tuning A value to achieve this sparsity
- When A = 0.005, there are 25% KC responding on average

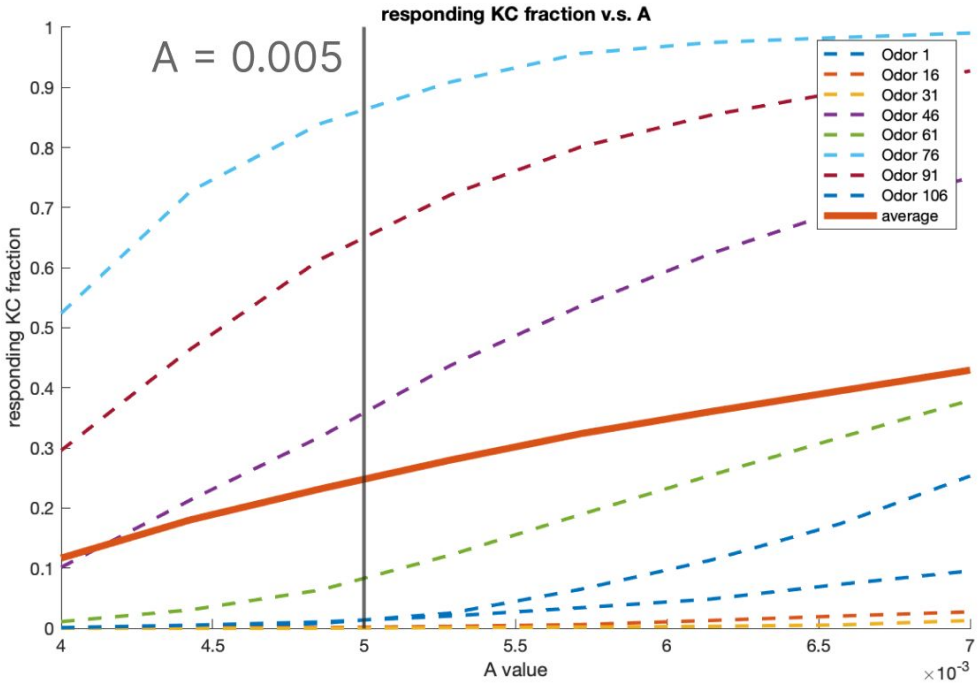

# Results

# Result 1: Local inhibition sparsen odor responses

The lifetime sparseness is measured by:

$$S_{KC} = \left(1 - \left(\left(\sum_{j=1}^{N} r_j/N\right)^2 / \sum_{j=1}^{N} {r_j}^2/N\right)\right)/(1 - 1/N)$$

- **N**: KC number
- $\mathbf{r_j}$: $KC_j$ spikes counts

If all KC respond to the odor homogeneously, $S_{KC} = 0$

## Sparse Responses

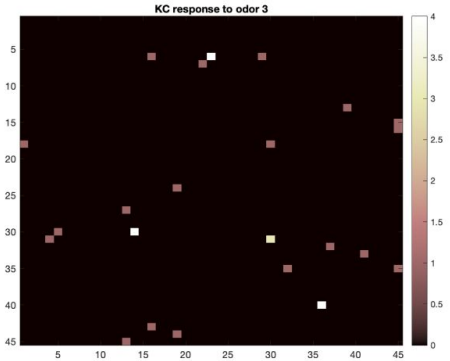


Responding KC: 1.14%
Lifetime Sparseness: 0.99

## Dense Responses

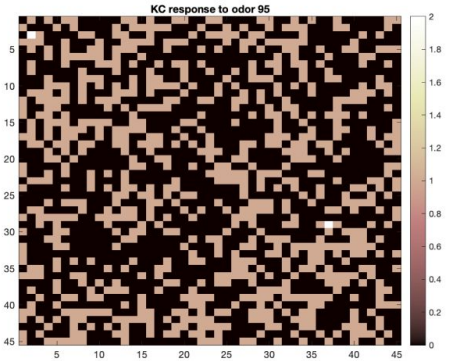


Responding KC: 38.77%
Lifetime Sparseness: 0.61

# Result 1: Local inhibition sparsen odor responses

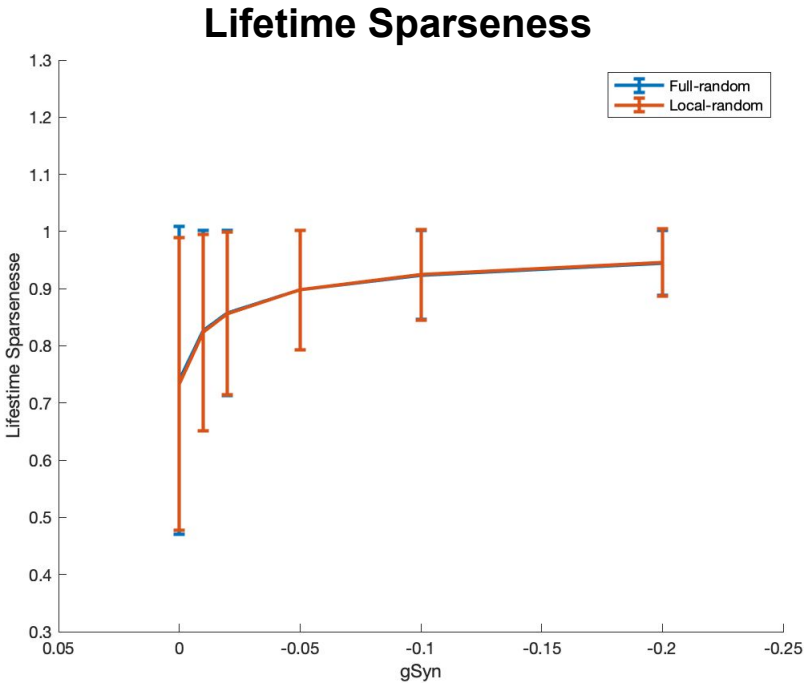


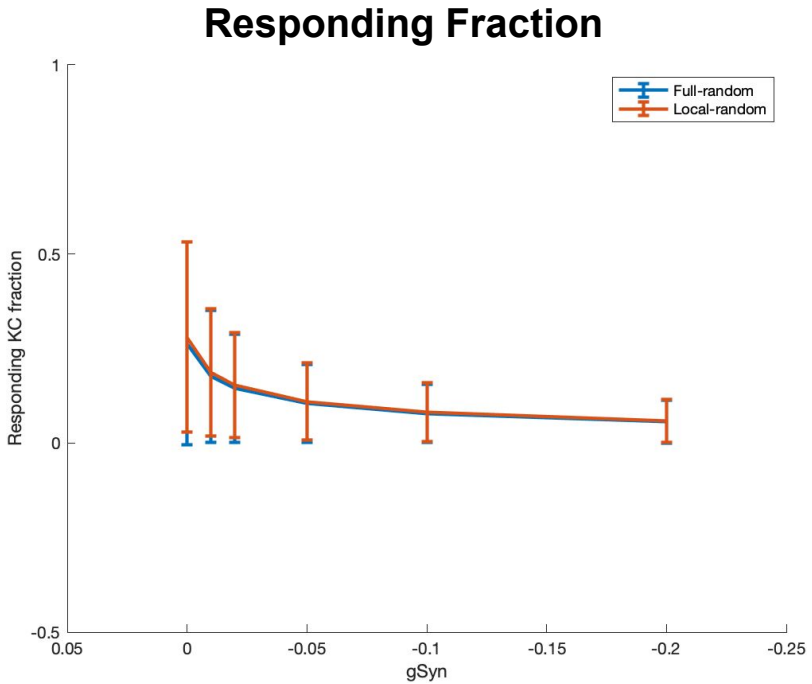


gSyn: Inhibition strength

A = 0.005, σ = 10, average of 110 odors

# Result 1: Local inhibition increases odor separability

- Simplified linear classifier
- ROC curve

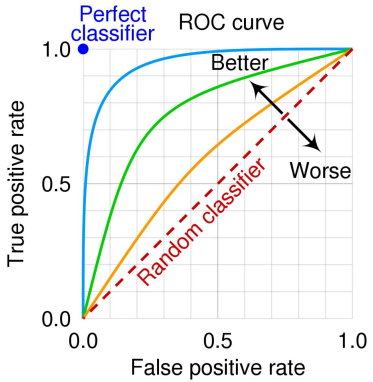


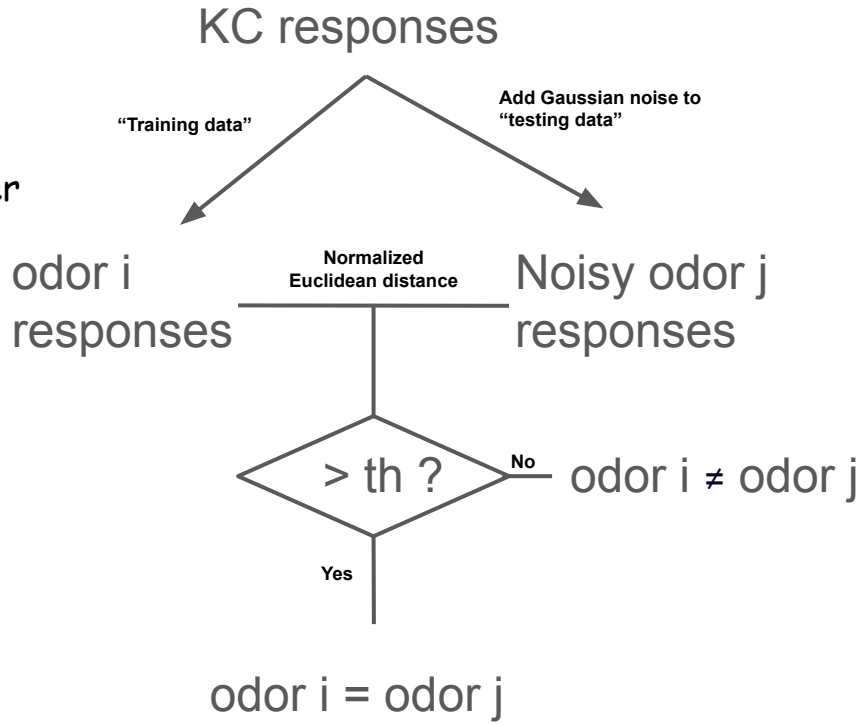


ROC figure:
https://medium.com/@ilyurek/roc-curve-and-auc-evaluating-model-performance-c2178008b02

# Result 1: Local inhibition increases odor separability

## Fully random PN-KC connection

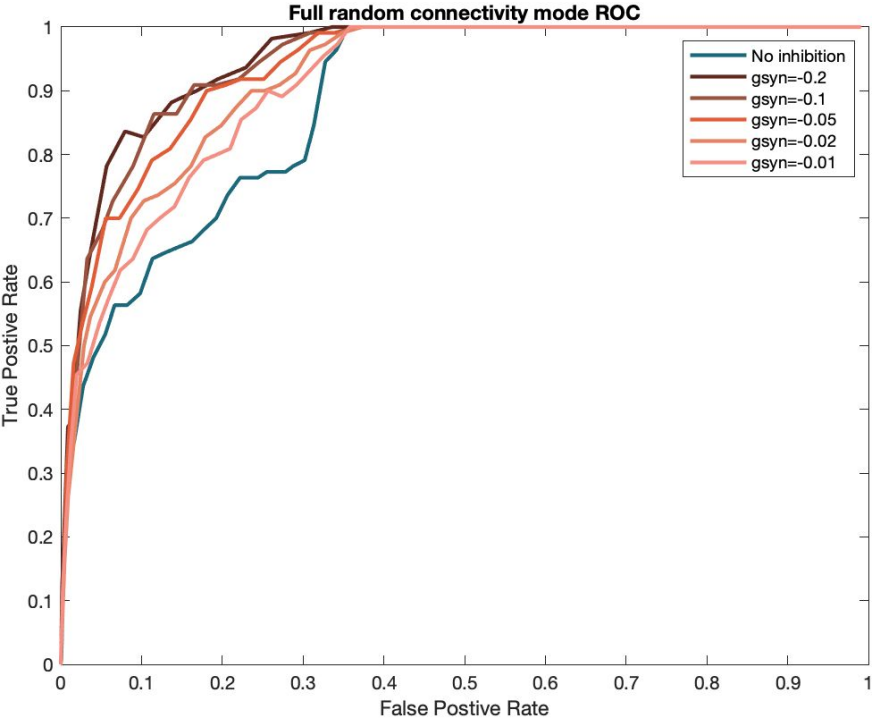


## Locally random PN-KC connection

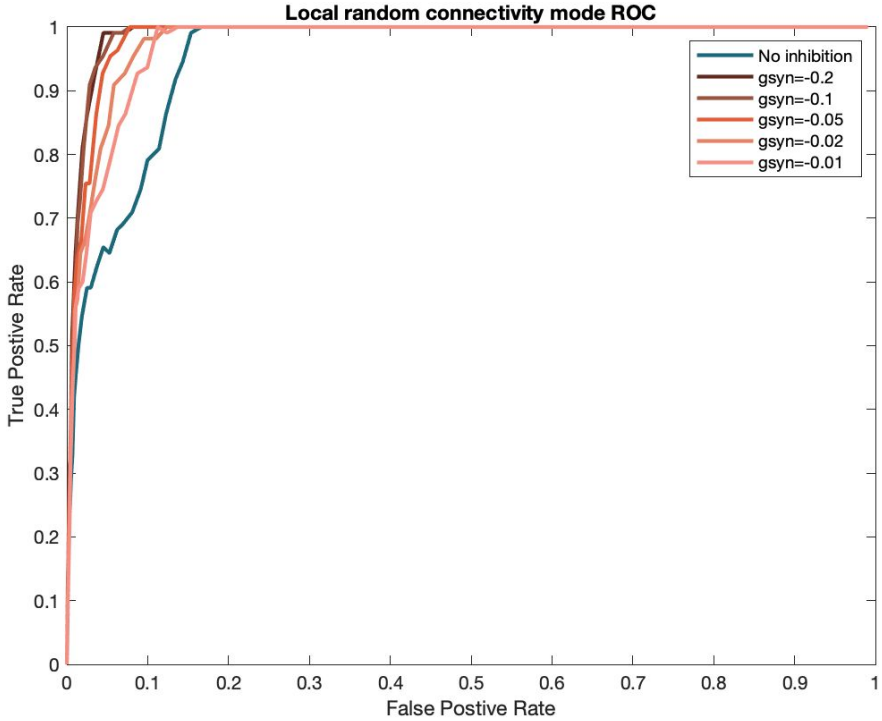

# Result 2: Exploring the effect of inhibition range

- To change inhibition range(σ), we control the sparsity of odor responses consistent. In Kennedy-MB model, APL will suppress KC responding fraction to 10%
- We randomly select 8 odors and tuning gSyn value to achieve this sparsity for each model with different inhibition range
- For the same sparsity, model with smaller inhibition range requires larger gSyn value

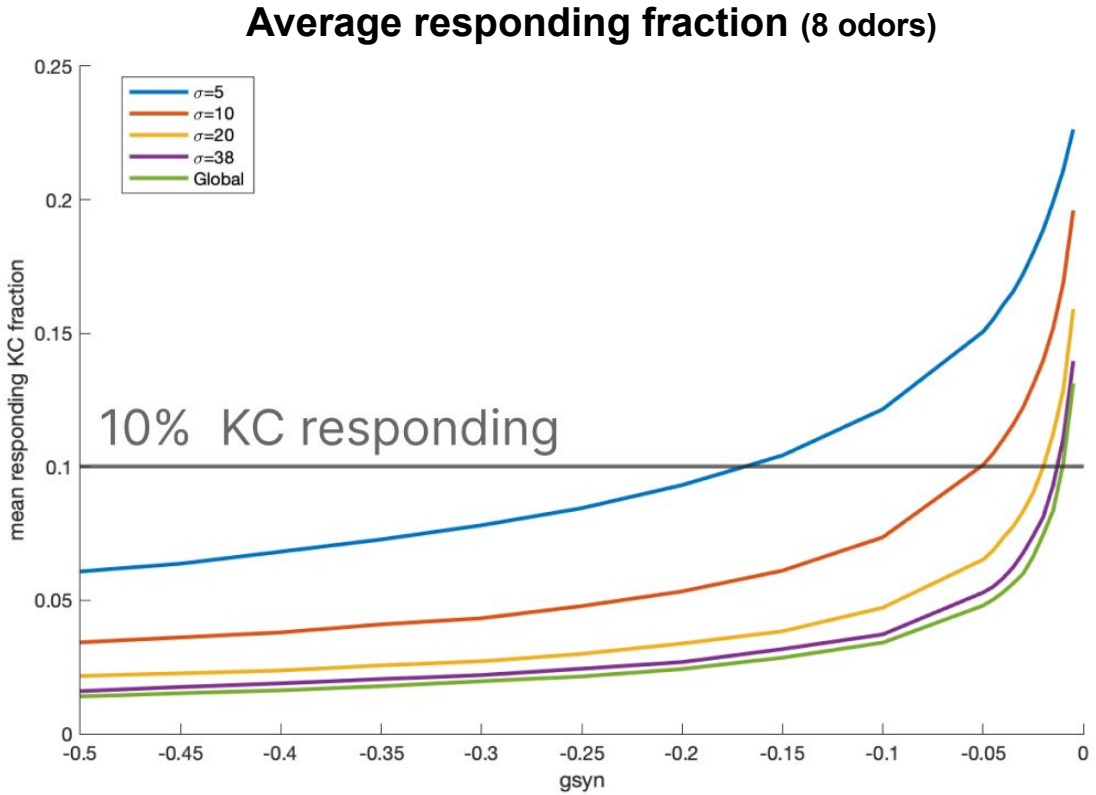

# Result 2: Exploring the effect of inhibition range

**Lifetime Sparseness**

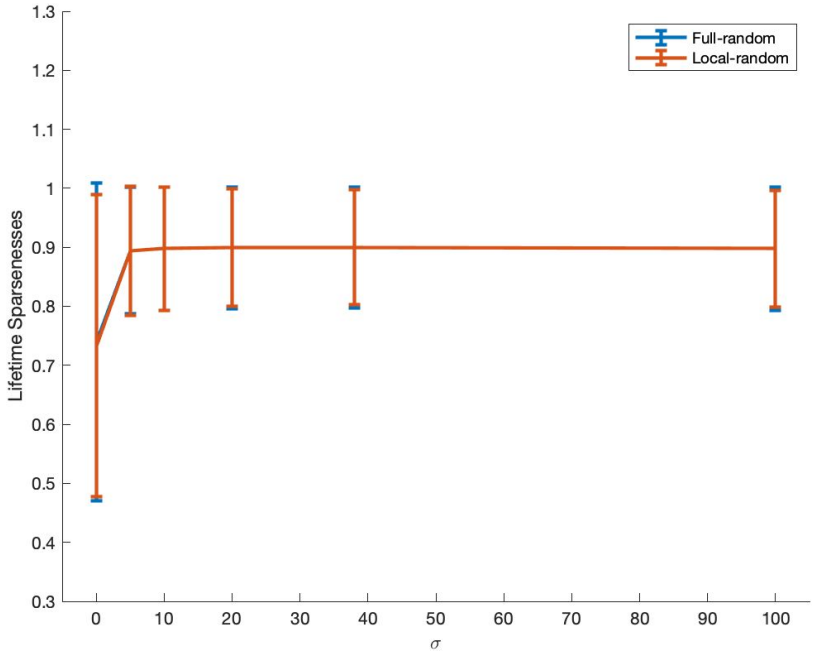


**Responding Fraction**

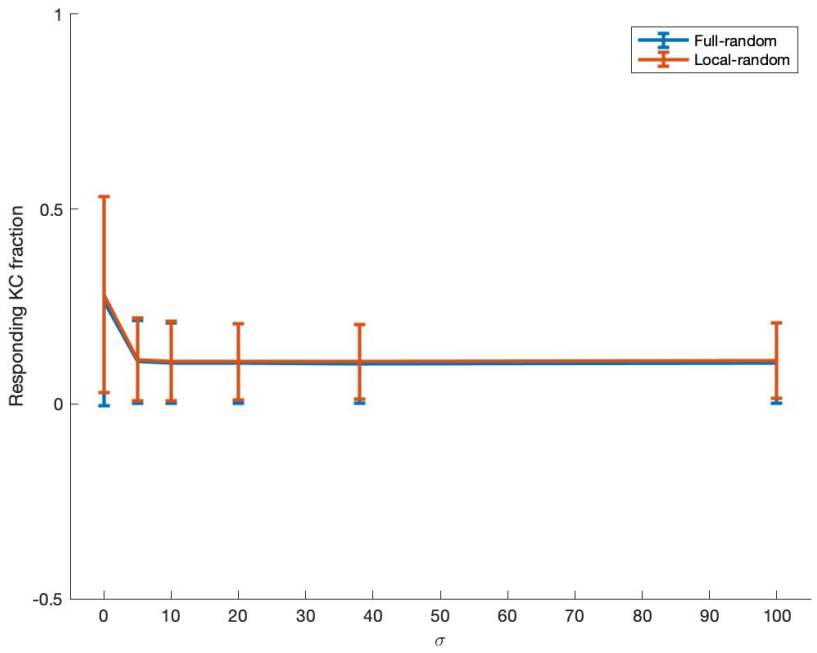


σ: Inhibition range

A = 0.005, average of 110 odors

# Result 2: Exploring the effect of inhibition range

## Fully random PN-KC connection

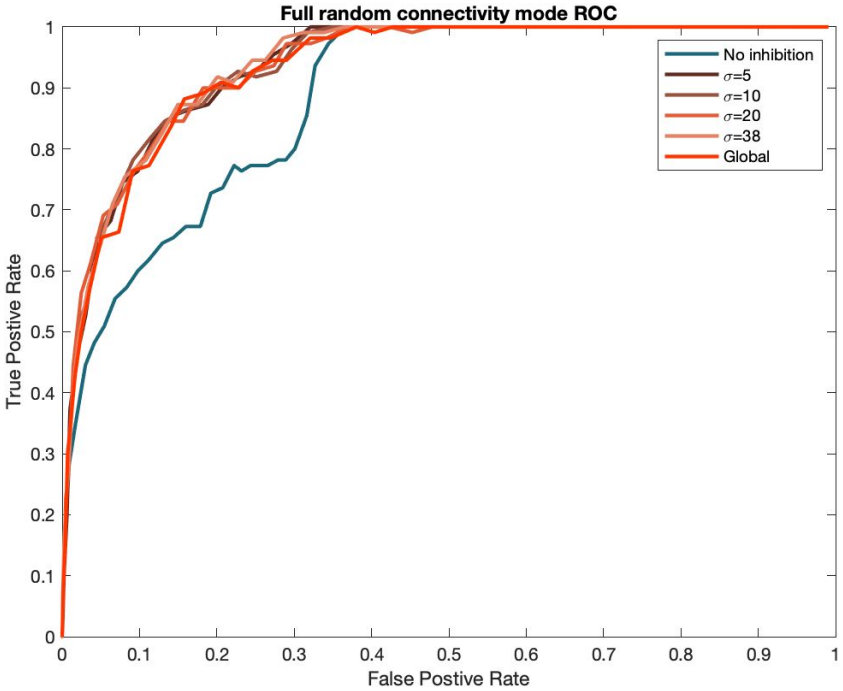


## Locally random PN-KC connection

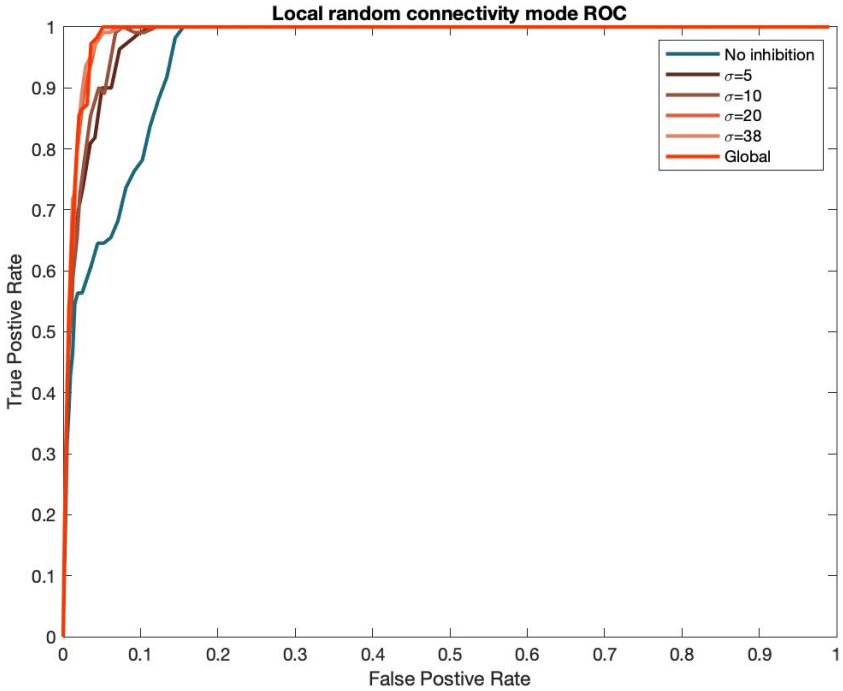

# Conclusion

- Local inhibition, a more realistic assumption based on recent findings, is able to perform on par with global inhibition models in regulating the sparsity of KC outputs
- Stronger inhibition will increase the sparsity, and make the odor representations more separable, hence the animal will be able to recognise the source odor with higher accuracy
- Controlling the sparsity and changing inhibition range do not alter prediction performance for full random PN-KC connectivity
- Local-random PN-KC connectivity improves the model performance compared to uniform/full random connectivity

**Through simulations, we have shown that a more physiologically realistic model is able to better predict the odors, and thereby explain the evolutionary advantage of its existence**

# Thank you!

Illustration courtesy: https://magazine.krieger.jhu.edu/fall-2021/humanitys-debt-to-the-lowly-fruit-fly/

# References


- [1] Cayco-Gajic, N. Alex, and R. Angus Silver. "Re-evaluating circuit mechanisms underlying pattern separation." Neuron 101.4 (2019): 584-602.
- [2] Luo, Liqun. "Architectures of neuronal circuits." Science 373.6559 (2021): abg7285.
- [3] Handler, Annie, et al. "Distinct dopamine receptor pathways underlie the temporal sensitivity of associative learning." Cell 178.1 (2019): 60-75.
- [4] Hige, Toshihide, et al. "Heterosynaptic plasticity underlies aversive olfactory learning in Drosophila." Neuron 88.5 (2015): 985-998.
- [5] Aso, Yoshinori, et al. "The neuronal architecture of the mushroom body provides a logic for associative learning." elife 3 (2014): e04577.
- [6] Lin, Andrew C., et al. "Sparse, decorrelated odor coding in the mushroom body enhances learned odor discrimination." Nature neuroscience 17.4 (2014): 559-568.
- [7] Scheffer, Louis K., et al. "A connectome and analysis of the adult Drosophila central brain." Elife 9 (2020): e57443.
- [8] Dorkenwald, Sven, et al. "FlyWire: online community for whole-brain connectomics." Nature methods 19.1 (2022): 119-128.

# References – contd.


- [9] Inada, Kengo, Yoshiko Tsuchimoto, and Hokto Kazama. "Origins of cell-type-specific olfactory processing in the Drosophila mushroom body circuit." Neuron 95.2 (2017): 357-367.
- [10] Amin, Hoger, et al. "Localized inhibition in the Drosophila mushroom body." Elife 9 (2020): e56954.
- [11] Aso, Yoshinori, et al. "Mushroom body output neurons encode valence and guide memory-based action selection in Drosophila." elife 3 (2014): e04580.
- [12] Li, Feng, et al. "The connectome of the adult Drosophila mushroom body provides insights into function." Elife 9 (2020): e62576.
- [13] Kennedy, Ann. "Learning with naturalistic odor representations in a dynamic model of the Drosophila olfactory system." bioRxiv (2019): 783191.
- [14] Hallem, Elissa A., and John R. Carlson. "Coding of odors by a receptor repertoire." Cell 125.1 (2006): 143-160.
- [15] Caron, Sophie JC, et al. "Random convergence of olfactory inputs in the Drosophila mushroom body." Nature 497.7447 (2013): 113-117.
- [16] Zheng, Zhihao, et al. "Structured sampling of olfactory input by the fly mushroom body." Current Biology 32.15 (2022): 3334-3349.